

The Non-linear Thin Shell Instability in Cloud–Cloud Collisions

Andrew D. McLeod and Anthony Peter Whitworth

Abstract Supersonic cloud–cloud collisions will produce a dense, shock-confined layer. This layer may be unstable to the non-linear thin shell instability (NTSI). We first explore the effect of different initial perturbations on the growth of the NTSI using smoothed particle hydrodynamics (SPH) simulations. We use one-dimensional monochromatic perturbations. We also use subsonic and supersonic turbulence to trigger the NTSI. We show partial agreement with the analytic predictions of Vishniac (ApJ 428:186, 1994). We then simulate a more realistic supersonic collision of molecular clouds with internal subsonic turbulence at a range of collision velocities. We show that at low collision velocity gravitational instability is dominant, but at higher collision velocities the NTSI becomes dominant and eventually suppresses star formation.

1 Introduction

Star formation occurs in dense gas. There are a range of physical processes that can collect gas in the Galaxy and raise its density. One such mechanism is converging flows, which lead to the formation of a shock-confined layer. Such collisions can occur from large-scale galactic flows [1–4], the collision of stellar winds [5] or supernovae bubbles [6], or turbulence on a range of scales [7].

A.D. McLeod (✉)
Astrophysics Group, School of Physics, University of Exeter, Stocker Road,
Exeter EX4 4QL, UK
e-mail: amcleod@astro.ex.ac.uk

A.P. Whitworth
Cardiff School of Physics and Astronomy, Cardiff University, Queens Buildings,
5 The Parade, Cardiff CF24 3AA, UK
e-mail: Anthony.Whitworth@astro.cf.ac.uk

Another mechanism is the supersonic collision of molecular clouds. We study the *non-linear thin shell instability* (NTSI), which occurs only in shock-confined layers [8]. The NTSI is a bending mode instability that enhances pre-existing perturbations in the layer.

Vishniac [8] derived the growth rate of the NTSI as a function of wavenumber, and found that $\tau^{-1} \propto k^{1.5}$ for one-dimensional monochromatic sinusoidal perturbations. We conduct simulations of the NTSI to demonstrate the analytic prediction of Vishniac. We also examine the instability in the collision of flows containing initial subsonic and supersonic turbulence. We then conduct more realistic simulations of cloud–cloud collisions, including self-gravity and a more complex equation of state.

2 Simulations of the NTSI

We conduct smoothed particle hydrodynamics (SPH) simulations of colliding flows using the Seren code [9] including hydrodynamics and artificial viscosity. We use an isothermal equation of state at 10 K, sound speed 0.19 km s^{-1} , and do not include self-gravity. The gas is initially of uniform density $10^{-21} \text{ g cm}^{-3}$, and the gas is set to collide at a Mach number \mathcal{M} of 20.

For one set of simulations we impose a one-dimensional monochromatic sinusoidal velocity perturbation, and repeat for a range of wavenumbers. We also create simulations containing subsonic and supersonic turbulence respectively.

2.1 Monochromatic Perturbations

Figure 1 shows the rate of growth of perturbations for simulations with monochromatic initial perturbations. At early times, the slope is small, as all wavenumbers are excited with an equal initial amplitude. As predicted, at later times larger wavenumbers grow faster. Figure 2 shows that after the initial rise, the slope of power law fits is somewhat higher than the predicted relation of $\tau \propto k^{1.5}$.

2.2 Turbulence

Figure 3 shows the rates of growth for simulations with turbulence. For supersonic turbulence, rates of growth decrease with increasing wavenumber, as the turbulence is strongest at small wavenumbers. There is no evidence of the NTSI. For subsonic turbulence, the turbulence still dominates at small wavenumbers, but at larger wavenumbers the NTSI dominates, leading to an increase in rates of growth at larger wavenumbers. This increase can be used as a diagnostic of the NTSI in simulations with turbulence.

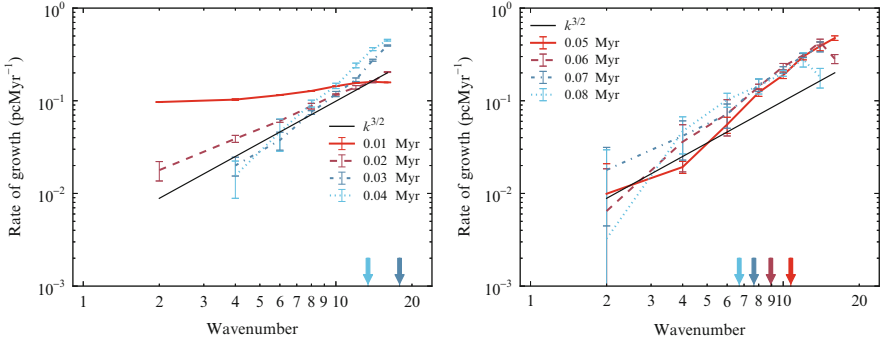
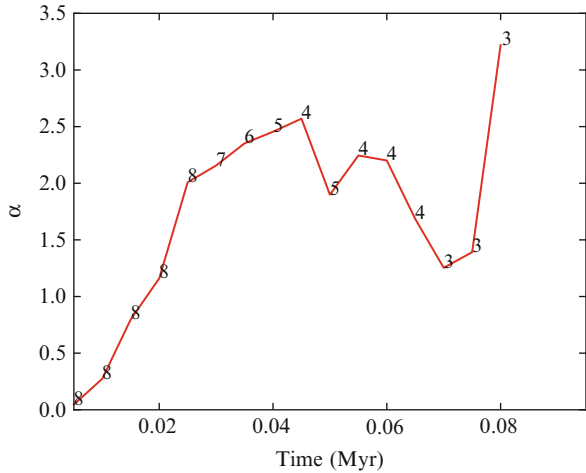


Fig. 1 The rates of growth for monochromatic perturbations as a function of wavenumber. Error bars show the standard deviation across realizations. The gradient of the *solid black line* indicates the relation predicted by Vishniac [8]. *Arrows* indicate the maximum resolvable wavenumber for the correspondingly coloured timestep; *arrows* run from latest to earliest timestep going left to right; some *arrows* are at larger wavenumbers than can be plotted

Fig. 2 Indices of power law fits to rates of growth of monochromatic perturbations as a function of time. The number of points used to construct each fit is also shown; fits constructed with fewer points are less reliable



3 Cloud–Cloud Collision Simulations

We simulate the supersonic collision of two $500 M_{\odot}$ clouds of uniform density $7 \times 10^{-22} \text{ g cm}^{-3}$ at a range of collision velocities. We include self-gravity, sink particles [10] and the Stamatellos [11] method to solve the energy equation. Each cloud contains subsonic turbulence with an average velocity of 0.1 km s^{-1} . Figure 4 shows no evidence for the NTSI for the low-velocity collision. The NTSI appears as a rise at larger wavenumbers for the high-velocity collision.

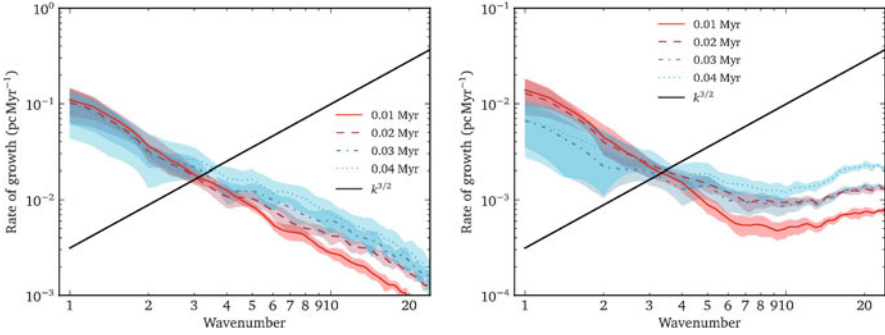


Fig. 3 Rates of growth of simulations with turbulence; as for Fig. 1. *Left*: supersonic turbulence; *right*: subsonic turbulence

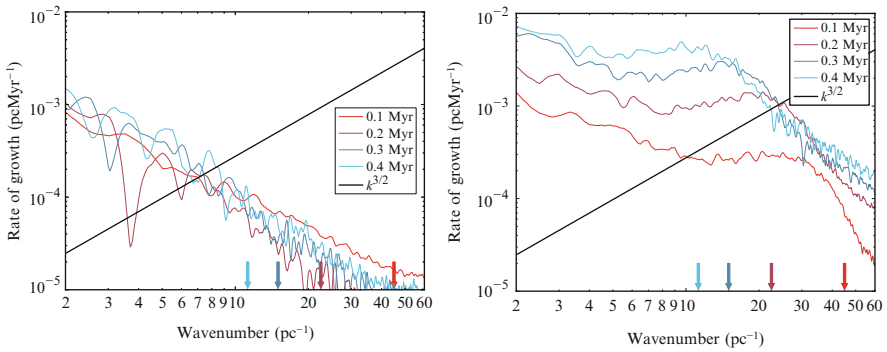


Fig. 4 Rates of growth for cloud–cloud collisions, as for Fig. 1. *Left plot* 1 km s^{-1} collision; *right plot* 5 km s^{-1} collision

4 Conclusions

We have explored the effect of the NTSI on dense shock-confined layers. Our simulations approximately match the analytic predictions of Vishniac [8]. We provide a qualitative diagnostic for the NTSI triggered by weak turbulence.

We simulate a realistic cloud–cloud collision at a range of collision velocities. As expected this produces a dense shock-confined layer. We find that at lower collision velocities the NTSI is not significant. At higher collision velocities the NTSI appears at higher wavenumbers.

References

1. I.A. Bonnell, C.L. Dobbs, T.P. Robitaille, J.E. Pringle, *MNRAS* **365**, 37 (2006).
2. E. Vázquez-Semadeni, D. Ryu, T. Passot, R.F. González, A. Gazol, *ApJ* **643**, 245 (2006).
3. F. Heitsch, L.W. Hartmann, A. Burkert, *ApJ* **683**, 786 (2008).
4. P. Hennebelle, R. Banerjee, E. Vázquez-Semadeni, R.S. Klessen, E. Audit, *A&A* **486**, L43 (2008).
5. I.R. Stevens, J.M. Blondin, A.M.T. Pollock, *ApJ* **386**, 265 (1992).
6. R.M. Williams, Y.H. Chu, J.R. Dickel, R. Beyer, R. Petre, R.C. Smith, D.K. Milne, *ApJ* **480**, 618 (1997).
7. M.M. Mac Low, R.S. Klessen, *Reviews of Modern Physics* **76**, 125 (2004).
8. E.T. Vishniac, *ApJ* **428**, 186 (1994).
9. D.A. Hubber, C.P. Batty, A. McLeod, A.P. Whitworth, *A&A* **529**, A27 (2011).
10. M.R. Bate, I.A. Bonnell, N.M. Price, *MNRAS* **277**, 362 (1995)
11. D. Stamatellos, A. Whitworth, T. Bisbas, S. Goodwin, *A&A* **475**, 37 (2007).